Monitoring the Impact of Urban Regeneration on Green Infrastructure: Istanbul Case

Ayşe Velioğlu*, Fatih Terzi
Affiliation: Istanbul Technical University, Faculty of Architecture, Department of Urban and Regional Planning, Istanbul, Turkey.
Email: velioglu22@itu.edu.tr, terzifati@itu.edu.tr

Abstract
This study examines the impact of urban regeneration projects carried out in Istanbul within the scope of Law No. 6306 on green infrastructure. The change in green infrastructure between 2014 and 2024 in three distinct regeneration sites was analysed using remote sensing, spatial texture analysis and machine learning techniques. NDVI, NDBI, and first-order statistical metrics derived from Landsat 8 satellite imagery are integrated into the change detection analysis using random forest classification. The findings show significant losses in green infrastructure, especially in areas where vertical densification is at the forefront. The results support that the level of integration of disaster-focused urban regeneration policies with climate adaptation and sustainability goals in the Istanbul case is limited, pointing to the need for more holistic planning approaches.

Keywords: urban regeneration; green infrastructure; NDVI; random forest; change detection

1. Introduction

Urban regeneration projects as transformative operations that strengthen and restructure the built environment under the risk of natural disasters have become one of the prior urban policies. These disaster-responsive projects aim to support resilience, contribute to sustainability, and increase the quality of life by optimizing the green infrastructure (Tzoulas et al., 2007; Wolch, Byrne and Newell, 2014). Green infrastructure is identified as a network of natural and semi-natural areas, including both green and blue spaces and it is part of the strategic planning approach for land conservation and optimized land use (Benedict and McMahon, 2006). It encompasses not only conserved natural areas, ecological corridors, urban drainages, and wetlands but also semi-natural, functional open spaces such as parks, farmlands, recreational sites, and greenways (Schilling and Logan, 2008; Fletcher et al., 2015). Also, as one of the main components of the urban ecosystem, green infrastructure supports adaptation to climate change (Oke, 1989; Spronken-Smith and Oke, 1999; Norton et al., 2015; Ramyar, Ackerman and Johnston, 2021). It helps mitigate the urban heat island effect, improve water and air quality, and manage stormwater, which are crucial for reducing the impacts of climate change and enhancing urban resilience (Nowak, Crane and Stevens, 2006; Meerow and Newell, 2017; Matasov et al., 2020; Senosiain, 2020; Halecki, Stachura and Fudała, 2025). Also, designing green infrastructure enhances city biodiversity by providing habitats for various species, contributing to ecological stability (Mathey et al., 2015; Pitman, Daniels and Ely, 2015). Apart from its advantages for the environment, green infrastructure is supposed to support public health, social cohesion, equity, and accessibility (Pauleit et al., 2019; Lu et al., 2023; Ogwu et al., 2025). Thus, green-driven urban renewal initiatives have evolved into useful instruments for resilience-oriented climate change adaptation policy (Gill et al., 2007; Semeraro, Aretano and Pomes, 2017). Supported by policy frameworks encouraging the use of green infrastructure, successful urban regeneration projects need the integration of resilience and sustainability ideas into urban agendas (Ignatieva and Mofrad, 2023; Zhang et al., 2025).

In Turkey, urban regeneration implementations are based on state law 6306 on the Regeneration of Areas at Disaster Risk. The main objective of the law is to constitute healthy and safe urban settlements (T. C. Resmi Gazete, 2012). Hence, the regeneration projects are recognised as opportunities for increasing sustainability in urban areas and developing climate-adaptive cities (Köylüoğlu, 2015; Yalazi et al., 2017; Korkmaz and Balaban, 2020; Yenidünya and Limoncu, 2024). By simulating possible risks such as flooding, the integration of the blue-green infrastructure systems in urban regeneration projects is highlighted as a strategy to adapt to climate change effect and improve urban resilience (Gündel and Kalaycı Önaç, 2025).

As a metropolitan city with vulnerable building stocks, Istanbul faces great seismic risk. Therefore, within the aim of law 6306, urban regeneration projects are operated as comprehensive planning tools in the city. According to the Istanbul Planning Agency's report (2023), after the law entered into effect, 70 urban areas have been declared as risky in Istanbul. Those risky areas correspond to about 2000-hectare urban settlements and 84,000 buildings at least. Policies for climate change mitigation and disaster mitigation-led urban regeneration have the potential to be conducted together. However, the actions for developing green infrastructure through regeneration projects are lower than expected (Kocabas, Gibson and Diren, 2015). Despite efforts to incorporate sustainability, the regeneration projects in Istanbul imply many speculative implementations, such as green gentrification, where green spaces become exclusive and inaccessible to the public (Yazar et al., 2020).

Contrary to the expectation of contributing to the quality of life by increasing the amount of green space in the city, preliminary findings show that urban regeneration projects implemented in areas declared risky have a diminishing effect on green spaces (Cengiz, Atmiş and Görmüş, 2019; Yağçı, 2025). Mostly, those projects result in higher density, and green spaces per cap remain inadequate. Limited empirical research focuses on how urban regeneration projects have influenced the green infrastructure in Istanbul over a long time. Addressing this issue, the study aims to investigate how urban regeneration projects based on law numbered 6306 impact the changes in urban green infrastructure. Under the green infrastructure umbrella, the study particularly focuses on urban green fabric as a projection of green infrastructure into the urban settlements, including all vegetation that can be observed in two dimensions by remote sensing, such as parks, urban forests, woodlands, grasslands, narrow green strips, street trees, green roofs, and green unfunctional spaces between buildings.

2. Material and Methods

In this study, a holistic method based on remote sensing and machine learning was designed to analyse the temporal change of urban green fabric in risky areas subjected to regeneration under law no 6306. Within the scope of the research, urban regeneration areas with sufficient data (n=21) were clustered, and three representatives from each cluster were selected as study areas. NDVI, NDBI, and first-order texture statistics were derived using Landsat 8 satellite multispectral images from 2014 and 2024 and clipped into those selected areas. These layers were composites into a multispectral raster mosaic for each year and random forest algorithm was used for the classification. As a final step, spatial transformations in green fabric were revealed through categorical change analysis over two years (Figure 1).

This methodological approach provides to evaluate the effects of urban regeneration practices on green fabric with objective data. It seeks to obtain accurate results through advanced spatial analysis that can direct policies for sustainable urban regeneration. In contrast to traditional planning methods, the use of machine learning techniques in this study enabled more optimised spatiotemporal analysis to address the complexity of urban space (Hoang and Tran, 2021; Jia, Cui and Liu, 2022; Rahaman et al., 2025).

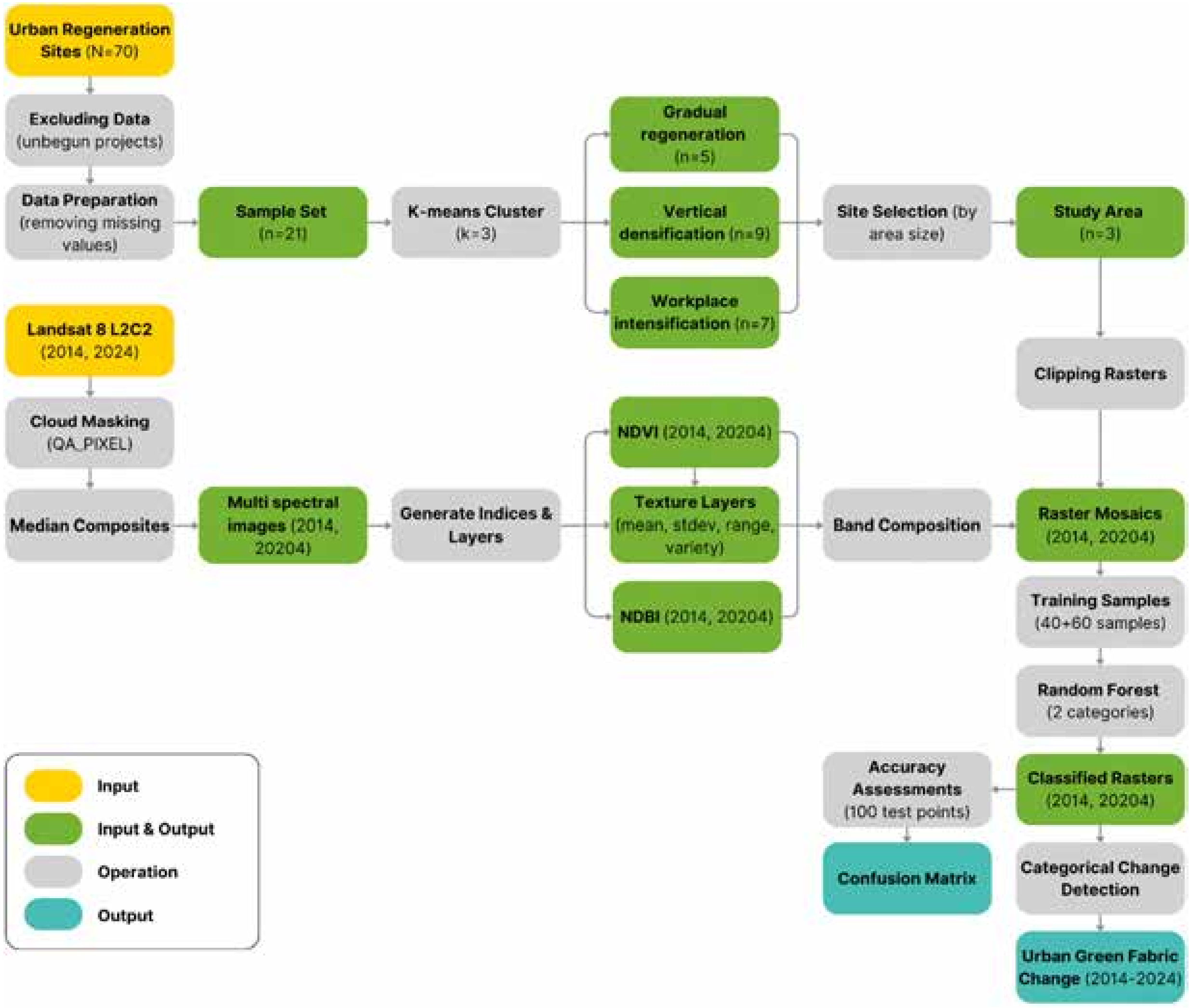

Figure 1. Workflow of the study.

2.1. Sample Selection and Study Area

Istanbul, one of the most highly populated and valued cities in Turkey, is in great seismic risk. By law 6306, 70 urban risk areas have been declared as urban regeneration sites in the city by the government (T. C. Resmi Gazete, 2012; Istanbul Planning Agency - IPA, 2023). This study focused on 25 projects which implementation has already begun of 70 declared urban regeneration sites, and 4 regeneration projects with missing data were excluded from the evaluation. Thus, 21 urban regeneration sites with sufficient data were accepted as the sample set (Table A. 1). To analyse the change in urban green fabric between 2014 - 2024 in different type of urban regeneration sites, k-means cluster analysis was applied with the logarithmic change rate of the following criteria below.

• Population capacity: the change in population capacity in the project area calculated before and after implementation
• Number of buildings: change in the number of buildings in the project area before and after implementation
• Number of workplace units: the change in the number of workplace units in the project area before and after implementation
• Gross construction area: the change of the total construction area in the project area before and after implementation

• Building renewals: the number of new buildings built for every building demolished during the implementation phase

Based on the Elbow score, regeneration sites have been clustered into three groups: (1) Gradual regeneration, (2) Vertical densification, and (2) Workplace intensification (Table 1).

Gradual regeneration represents areas with relatively low intervention levels, with values below the average in log-ratio-based indicators. Negative ratios in the number of buildings (-0.64) and gross construction area (-0.28) indicate that regeneration has been conducted gradually. The decrease in the number of workplaces (-0.37) indicates that the regeneration process in these areas is progressing with a priority on housing and away from functional diversity. In addition, the building renewal rate is also quite low (-1.96), which may indicate that the regeneration is more in the "processing" stage (Yazar et al., 2020).

On the other hand, vertical densification stands out with radical reconstruction and urban fabric densification practices. The construction area change rate (+2.47) indicates that parcels are combined to produce larger buildings. While the number of buildings is decreasing (-1.56), the increase in population capacity (+0.64) and the number of workplaces (+0.21) is a distinct indicator of vertical growth and mixed-use developments. The low rate of building renewal (-2.41) shows that the regeneration model in these areas is not "renewal" but entirely redevelopment-based. This cluster covers areas mostly high-investment, densely populated, and open to speculative development, which are symbolic examples of urban regeneration discussions in Istanbul (Turk, Tarakci and Gürsoy, 2020).

Workplace intensification defines the areas where the regeneration process is shaped towards gaining trade and services function. The workplace unit change rate is quite high (+4.03). This situation shows that existing housing or empty buildings are transformed into new function or mixed structures are built with commercial layers. Population growth (+0.98) and an increase in construction areas (+1.22) support this regeneration. Although the building renewal rate is relatively low (-1.36), it points to a scenario where functional transformation is preferred instead of dense construction.

Following cluster analysis, the urban regeneration site with the largest area size from each cluster was selected as a representative so that the classification analysis (random forest) could be applied in the study and yield reliable results (Figure 2). Features of designated study areas, cluster centre distances, and area sizes are given in Table 2 and Table 3.

• Site – 1: Karabekir, Fevziçakmak project site is located on the east side of Gaziosmanpaşa district (41°5′7″ N - 41°5′46″ N, 31°54′17″ E - 31°54′58″ E). The regeneration has started in 2017; it is still in the early stages of demolition and reconstruction (Figure A. 1). Based on the capacity population before the regeneration project, the total construction area per capita was 41 m2, and it is expected that the construction area per capita will decrease by 12% and become 36.21 m2 after the project. This regeneration site is one of the highly representative samples of the gradual regeneration cluster.

• Site – 2: Fikirtepe project site is located at centre of Kadıköy district near to D100 highway (41°0′17″ N - 41°0′18″ N, 32°2′36″ E - 32°4′15″ E). The project's start date was 2012 (Figure A. 1). While the total construction area per capita based on the capacity population was 22.33 m² before the regeneration project, this value is expected to increase by 473% and reach 128 m² after the project based on the planned capacity population. This situation indicates a remarkable increase in the building density. The project strongly represents a vertical densification cluster.

• Site – 3: Çınar, İnönü, Sancaktepe, Yavuzselim, Merkez project site is located in the south-east of Bağcılar district (41°2′56″ N - 41°3′11″ N, 31°51′7″ E - 31°51′33″ E). The beginning date of the implementations was 2013 (Figure A. 1). While the total construction area based on the capacity population before the project was 65.09 m2, the construction area per capita is expected to decrease by 32% and become 44.21 m2 based on the planned capacity population after the project. The regeneration site is a moderate-represented member of the commercial intensification cluster; however, it is the only project site with a considerable area size for the classification.

Table 1: Attributes of urban regeneration zones.

Average Change Rates					
Clusters	Population capacity	Buildings	Workplace units	Construction area	Renewals
Gradual regeneration	0.14	-0.64	-0.37	-0.28	-1.96
Vertical densification	0.64	-1.56	0.21	2.47	-2.27
Workplace intensification	0.98	-0.93	4.03	1.22	-1.36

Figure 2. Study Areas in 2024: (a) Site – 1; (b) Site – 2; (c) Site – 3.

Table 2. Features of the selected study areas.

Indicators	Rates of Change Between Periods		
	Site - 1	Site - 2	Site - 3
Population capacity	0.295	0.556	0.685
Number of buildings	-0.082	-1.568	-0.185
Number of workplace units	-0.256	-0.063	6.895
Gross construction area	0.170	2.302	0.298
Building renewals	-1.686	-3.112	-2.114

Table 3. Cluster representation of the selected study areas.

Regeneration Site	Cluster No	Cluster Centre Distance	Area Size (Ha)
Karabekir, Fevziçakmak - Gaziosmanpaşa	1	0.788	59.03
Fikirtepe - Kadıköy	2	0.901	98.73
Çınar, İnönü, Sancaktepe, Yavuzselim, Merkez - Bağcılar	3	3.204	22.07

2.2. Satellite Images and Data Processing

Landsat 8 surface reflectance images (Collection 2, Level-2) were used for 2014 and 2024 to classify urban green fabric in regeneration sites. Based on the project start date of selected regeneration sites, the oldest year, one year after Landsat 8 was launched, has been selected as the reference year. The image data was obtained from the Google Earth Engine platform. Cloud-free composite images were generated by applying a pixel-based median compositing technique after cloud masking with the QA_PIXEL band. After filtering out low-quality pixels, annual median composites were generated by taking the median reflectance values from all valid images within each two years. All images were clipped to the Istanbul metropolitan area and exported at 30-meter resolution in EPSG:4326 projection (41.0082° N, 28.9784° E).

NDVI was used as the basis to analyse urban green fabric in Istanbul regeneration sites. For more accurate classification, NDVI was supported with NDBI and texture layers. The pre-classification process (clipping, band composition, etc.) and advanced analysis were conducted in ArcGIS Pro 3.1.

NDVI Calculation

NDVI is a well-accepted index to quantify vegetation in urban areas by comparing reflectance values in the red and near-infrared (NIR) spectral bands (Weng, Lu and Schubring, 2004; Yuan and Bauer, 2007; Feyisa, Dons and Meilby, 2014). It helps to identify vegetation density, vegetation health, and developed areas. The NDVI value ranges from -1 to 1; an upper value than 0.2 refers to vegetation cover. The index is also useful in spatiotemporal analysis and monitoring the vegetation change over time (Jeevalakshmi, Reddy and Manikiam, 2016; Luo et al., 2021). Here, NDVI was generated from Landsat 8 multispectral image data for 2014 and 2024. The calculation is as follows:

$$NDVI = \frac{\rho_{nir} - \rho_{red}}{\rho_{nir} + \rho_{red}} \qquad (1)$$

Where p_{nir} and p_{red} represent the red reflected radiant flux (Band 4, 0.64 - 0.67 µm) and near-infrared radiant flux (Band 5, 0.85 - 0.88 µm) respectively. However, granular surfaces in urban areas with high heterogeneity may have similar NDVI values. NDBI and texture layers were also used to avoid this misleading and to facilitate the discrimination of low vegetation areas such as parks, gardens, and grasslands from built-up areas (Haralick, Dinstein and Shanmugam, 1973; He et al., 2010).

NDBI Calculation

The primary use of NDBI is to map and monitor urban built-up areas. It also combines with NDVI to distinguish vegetation from built-up areas. It ranges from -1 to 1, and similarly to NDVI, positive values indicate built-up areas (Zha, Gao and Ni, 2003; Bhatti and Tripathi, 2014). NDBI addresses the challenge of distinguishing urban areas from bare ground and providing more accuracy in identifying urban green fabric. Hence, its combination with NDVI especially assists in separating barren land from urban areas (He et al., 2010). NDBI is computed as below:

$$NDBI = \frac{\rho_{swir} - \rho_{nir}}{\rho_{swir} + \rho_{nir}} \quad (2)$$

Where p_{swir} and p_{nir} represent the short-wave infrared - 1 reflected radiant flux (Band 6, 1.57 - 1.65 μm) and near-infrared radiant flux (Band 5, 0.85 - 0.88 μm) respectively.

Texture Analysis

Texture analysis in image processing is effectively used to classify vegetation in urban areas. As one of the texture extraction methods, the grey-level co-occurrence matrix (GLCM) captures the spatial relationship between pixel pairs in an image, reflecting the texture by considering the direction, distance, and magnitude of changes in grayscale values (Haralick, Dinstein and Shanmugam, 1973; Gao et al., 2015; Yan, Shaker and El-Ashmawy, 2015). The method has been used to extract texture features from high-resolution satellite images to classify various types of urban vegetation, such as parks, street trees, grasslands, and scrub vegetation (Liu and Yang, 2013). Combining GLCM with spectral indices significantly improves the classification accuracy of green fabric in urban areas (Wu et al., 2019). Alternative to GLCM, some research measures texture using histograms based on the sum and difference of pairs of pixels (Unser, 1995; Sarker and Nichol, 2011). Other researches argue that geostatistical texture metrics provide more accuracy in classification (Rodriguez-Galiano, Chica-Olmo, et al., 2012).

Although texture measures such as GLCM and geostatistical-based metrics can improve classification accuracy, they require increased computational demands and higher data dimensionality (Pacifici, Chini and Emery, 2009; Ghimire, Rogan and Miller, 2010; Sarker and Nichol, 2011). In this study, first-order statistical descriptors (mean, standard deviation, range, and variety) were used instead. They offer an efficient alternative with adequate discriminatory power for medium-resolution imagery.

Here, first-order statistical metrics were derived from the NDVI raster using the Focal Statistics tool in ArcGIS Pro. These metrics included mean, standard deviation, variance, and range – each calculated over a 7×7 moving window (Franklin et al., 2000; Kayitakire, Hamel and Defourny, 2006): (i) Mean represents the local green density where x_i is for each pixel value and N for total number of pixels; (ii) Standard deviation reflects surface heterogeneity and variation where μ is for mean, x_i for each pixel value and N for total number of pixels; (iii) Range was used to identify environmental transition areas, indicating structural contrast where x_i stands for each pixel value; and (iv) Variety counts how many different pixel values are in the neighbourhood window. It measures diversity like "entropy" in GLCM but in terms of class diversity, not randomness (Table 4).

Table 4. Texture layers calculation.

Texture ayers of NDVI	Raster Calculation	GLCM Calculation
Meanv	$\frac{1}{N}\sum_{i=1}^{N} x_i$	-
Standard deviation	$\sqrt{\frac{1}{N}\sum_{i=1}^{N}(x_i-\mu)^2}$	-
Range (contrast)	$max(x_i) - min(x_i)$	$\sum_{i,j}(i-j)^2 . P(i,j)$
Variety (entropy)	$UniqueClasses(x_i)$	$-\sum P(i,j).\log_2 P(i,j)$

2.3. Green Fabric Classification and Accuracy Assessments

This study performed a random forest classifier to distinguish between urban green fabric and built-up areas in urban regeneration sites. This technique offers high accuracy rates in different image data (Rodriguez-Galiano, Ghimire, et al., 2012; Talukdar et al., 2020) and gives balanced performance in both homogeneous and heterogeneous land cover classes (Shi and Yang, 2017). Studies have shown that random forest-based classification is suited for reducing the data dimensionality of complex urban land cover types while reserving discrimination of different classes (Gan et al., 2016; Isaac, Easwarakumar and Isaac, 2017). It is also robust to reductions in training data size and noise (Rodriguez-Galiano, Ghimire, et al., 2012) and the risk of overfitting by averaging the predictions of multiple decision trees (Gislason, Benediktsson and Sveinsson, 2006).

As detailed in Section 2.2, NDVI, NDBI, and texture layers generated from NDVI were computed separately and composed into a multispectral image for each year. Due to the radiometric inconsistencies observed in parts of the 2014 Landsat 8 image, particularly in non-urban northern-east regions, the classification process was restricted to the regeneration project boundaries. This spatial constraint minimizes the uncertainty introduced by low observation density and ensures that the classification model is trained and applied to radiometrically stable regions.

Two main classes were determined to run random forest classifications: urban green fabric and built-up area. The training data were manually selected from the composited multispectral images. For both classes, sample polygons were determined by considering clearly separated areas, and pixel samples were taken from these regions for two images. The samples were collected individually for both years. The class distribution of the training samples was determined in parallel with the existing spatial ratios in the study area; 40% of samples were used for the urban green fabric class, and 60% of them were used for the built-up area class.

Classification results for 2014 and 2024 show that the model is adequately accurate (Table 5 and Table 6). In 2014, the overall accuracy was 84%, and the kappa statistic was 0.68; in 2024, these values were 85% and 0.70%, respectively. For both years, the built-up area class performed very strongly regarding user accuracy (94% and 98%), demonstrating the model's ability to correctly identify built-up areas. The urban green fabric class performed relatively low in user accuracy (74% and 72%) despite high producer accuracy values (92.5% and 97%). The relatively low user accuracy in the urban green fabric class indicates that some class assignments may be inaccurate when classifying small and fragmented urban areas using satellite imagery with a spatial resolution of 30 meters. This is related to the lack of clear spectral separation of green areas that have been transformed or are simply intersected with buildings, making them hard to identify. However, given the overall accuracy of the model (84-85%) and the kappa statistics (0.68-0.70), this limitation does not undermine the overall reliability of the classification results. It reveals that the outputs obtained are acceptable (Figure 3).

Table 5. Accuracy assessment of green fabric classification for 2014.

	Built-up Area	Green Fabric	Total Count	User's Accuracy
Built-up Area	47	3	50	0.94
Green Fabric	13	37	50	0.74
Total Count	60	40	100	0
Producer's Accuracy	0.78	0.925	0	0.84
Kappa Statistics: 0.68				

Table 6. Accuracy assessment of green fabric classification for 2024.

	Built-up Area	Green Fabric	Total Count	User's Accuracy
Built-up Area	49	1	50	0.98
Green Fabric	14	36	50	0.72
Total Count	63	37	100	0
Producer's Accuracy	0.77	0.97	0	0.85
Kappa Statistics: 0.70				

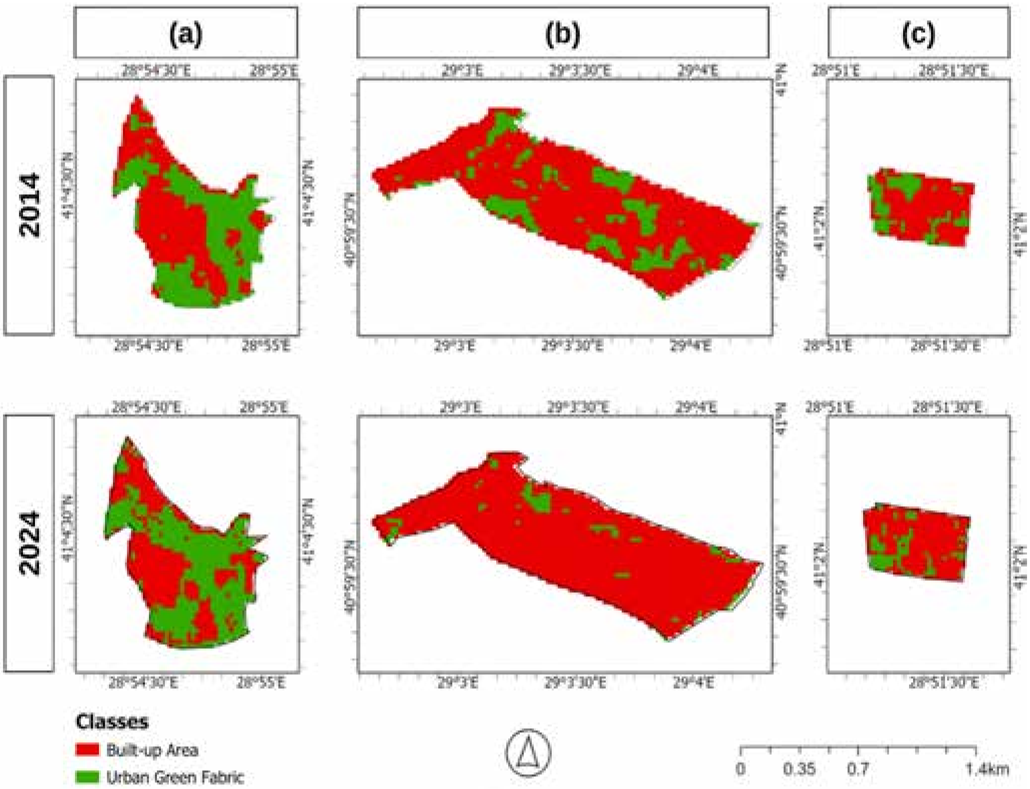

Figure 3. Urban green fabric classification in 2014 and 2024: (a) Site – 1; (b) Site – 2; (c) Site – 3.

3. Urban Green Fabric Change in Regeneration Sites

To analyse the change of green fabric in selected regeneration sites between 2014 and 2024, categorical change detection was processed with defined classes of urban green fabric and built-up areas. In order to suppress pixel-level random noise in the classification results and to ensure spatial consistency in the change map, a 3×3 smoothing neighbourhood window was used, and the median was preferred as the statistical filling method. This configuration reduces the effect of random pixel fluctuations in fragmented and small-scale urban green areas, allowing for more reliable and coherent change detection (Chen, Stow and Gong, 2004; Ghimire, Rogan and Miller, 2010).

The findings show that remarkable spatial changes were observed in the three representative urban regeneration sites between 2014 and 2024 (Figure 4). In Site – 1, which represents a gradual regeneration cluster, there is a 9.18% increase in green fabric, accompanied by a 9.43% loss of building development (Table 7). Since regeneration interventions are still in process and reconstruction not being completed substantially, the increase in green fabric cannot be interpreted as final result unlike in the other two regeneration sites (Figure A. 1). The green fabric per capita decreased from 21.47 m2 to 17.45 m2 by the planned population capacity (Table 7 and Table 8). Based on the current population in 2023, the amount of green fabric per capita is 58.56 m2. This current high ratio supports the inference about ongoing reconstruction process.

Site – 2, as a strong member of the vertical densification cluster, reveals an intensified urban regeneration process, exhibiting an increase of 18.42% in buildings with a very high green fabric loss of 74.15% (Table 7). During the regeneration process, this area has come under intense building pressure and exhibited a negative picture regarding environmental sustainability and life quality. According to planned population capacity, green fabric per cap has dramatically decreased from 4.61 m2 to 0.68 m2. Also, the current green fabric per cap is 3.07 m2 (Table 7 and Table 8). These rates are significantly below the World Health Organization's (WHO) minimum rate – 9 m2 (World Health Organization - WHO, 2012).

As a member of the workplace intensification cluster, in Site – 3, the building rate increased by 11.7%. In comparison, the green fabric decreased by 28.79%, indicating that the green fabric was largely transformed into built-up areas (Table 7). Here, it should be considered that Site – 3, which has been selected due to its optimal area size, has relatively low cluster representation; so, similar rates may not be seen in other areas where functional transformation has occurred. During the regeneration, green fabric per capita has decreased from 18.85 m2 to 6.76 m2. As seen in Table 7 and Table 8, the current rate is more negative than the planned one; green fabric per capita is 4.94 m2 by the population in 2023. Considering the functional transformation of the project, it is expected that some of the current population will be replaced. However, according to WHO's minimum limit, planned green fabric per capita is still lower than the rate before the regeneration (World Health Organization - WHO, 2012; Russo and Cirella, 2018).

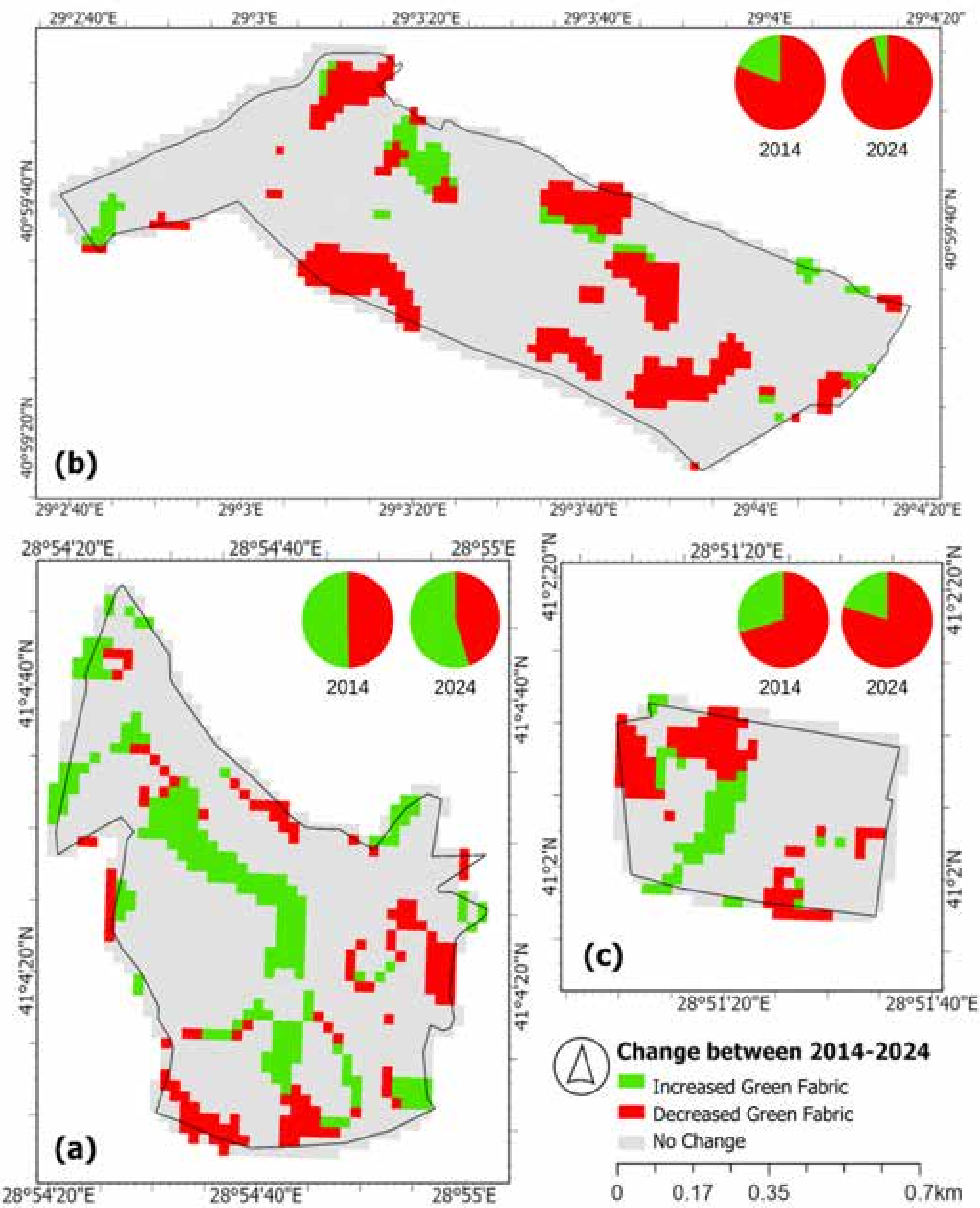

Figure 4. Urban green fabric changes in selected regeneration sites between 2014- 2024: (a) Site – 1; (b) Site – 2; (c) Site – 3.

Table 7. Change in urban green fabric between 2014-2024.

Project Site	Area Size						Change Rate (%)		
	2014			2024					
	Built-up (ha)	Green Fabric (ha)	Green Fabric per cap (m2)	Built-up (ha)	Green Fabric (ha)	Green Fabric per cap (m2)	Built-up	Green Fabric	Green Fabric per cap
Site - 1	28.73	29.23	21.47	26.02	31.92	17.45	-9.43	9.18	-18.58
Site - 2	77.17	18.66	4.61	91.38	4.82	0.68	18.42	-74.15	-85.24
Site - 3	15.50	6.34	18.85	17.31	4.51	6.76	11.70	-28.79	-64,13

Table 8. Changed population in regeneration sites.

Project Site	2014		
	Population Capacity		Current Population
	Pre-regeneration	Post-regeneration	
Site - 1	13615	18291	5451
Site - 2	40439	70563	15681
Site - 3	3363	6674	9129

4. Conclusion

This paper investigates the spatial change in urban green fabric between 2014 and 2024 using three representative areas in Istanbul subjected to urban regeneration policies under law no. 6306. Combining NDVI, NDBI, and texture-based statistics with random forest classification reveals the different effects of various regeneration strategies on green areas in the analysis. Notably, the vertical densification cluster experienced a drastic decline of 74.15% in green fabric, highlighting the conflict between intensive redevelopment and environmental sustainability. The workplace intensification site also experienced a significant transition from green to built-up zones (28.79%). In contrast, the gradual regeneration cluster showed a moderate increase in green areas. However, this increase in green fabric detected based on NDVI should not be interpreted as a final conclusion comparable to the other two regeneration sites since construction activities are largely incomplete in Site-1 (in Gaziosmanpaşa). The decrease in planned green fabric per capita in post-regeneration of Site -1, as shown in Table 7, supports this caution. In all areas, the amount of green fabric per capita (based on the planned capacity population) after regeneration remained below the pre-regeneration era. Additionally, current rates in Site – 2 (in Kadıköy) and Site – 3 (in Bağcılar) are lower than the minimum value recommended by the WHO.

Although law no. 6306 aims for healthy and safe urban settlements, the findings show that it remains insufficient in terms of protecting or increasing green fabric during the implementation phase. The spatial decrease in urban green fabric in different regeneration clusters emphasize the decisive role of planning strategies on ecological and climate-adaptive outcomes. However, it should be noted that the negative change in the urban green fabric detected through remote sensing and advanced spatial analysis cannot be evaluated only in two-dimensional spatial criteria that are reduced to urban settlement. Urban green fabric functions as a part of a regional green infrastructure that includes urban elements (parks, street trees, gardens, etc.) as well as forests, agricultural areas, riparian zones, and wide-open spaces outside the city. Although these urban periphery natural elements are located outside urban settlement areas, they directly affect the quality of urban life by providing critical ecosystem services such as improving air quality, providing biodiversity corridors, climate regulation, and groundwater recharge. Therefore, changes in the urban green fabric should also be evaluated in the context of the continuity and integrity of the holistic green infrastructure network, not limited to urban borders. Accordingly, there is a need for multi-dimensional planning approaches that integrate disaster-focused response objectives with climate adaptation and urban ecology. Green infrastructure should be considered a holistic planning component in regeneration areas and a fundamental precondition for building sustainable and resilient cities.

Although this study proposes a powerful method based on remote sensing and machine learning, it has some limitations. First, to improve classification accuracy, the regeneration project with the largest area from each cluster was selected as a representative. However, this choice may have weakened how well some clusters are represented. Second, the 30-meter spatial resolution of Landsat 8 imagery may be insufficient to detect small-scale green areas like narrow strips, street trees, or green roofs. Although NDVI, NDBI, and texture statistics were used to improve classification accuracy, spectral similarities between low-density vegetation and built-up areas may still cause confusion. Additionally, first-order statistics (mean, std, range, variance) were used instead of second-order metrics like GLCM to describe spatial texture, which reduced computational cost but also limited detailed discrimination. Third and finally, the analysis only covers the years 2014 to 2024, so it cannot fully reflect all temporal changes, regeneration stages, or land use transitions during the ongoing projects. This may lead to temporary vacant areas or unbuilt parcels between new buildings being misleadingly perceived as green fabric on NDVI. Future studies can address these limitations by using higher-resolution data, time series analysis, and field observations.

5. References

Benedict, M.A.. and McMahon, Edward. (2006) Green infrastructure: linking landscapes and communities. Washington: Island Press.

Bhatti, S.S. and Tripathi, N.K. (2014) 'Built-up area extraction using Landsat 8 OLI imagery', GIScience and Remote Sensing, 51(4), pp. 445–467. Available at: https://doi.org/10.1080/15481603.2014.939539.

Cengiz, S., Atmiş, E. and Görmüş, S. (2019) 'The impact of economic growth oriented development policies on landscape changes in Istanbul Province in Turkey', Land Use Policy, 87. Available at: https://doi.org/10.1016/j.landusepol.2019.104086.

Chen, D., Stow, D.A. and Gong, P. (2004) 'Examining the effect of spatial resolution and texture window size on classification accuracy: An urban environment case', International Journal of Remote Sensing, 25(11), pp. 2177–2192. Available at: https://doi.org/10.1080/01431160310001618464;WGROUP:STRING:PUBLICATION.

Feyisa, G.L., Dons, K. and Meilby, H. (2014) 'Efficiency of parks in mitigating urban heat island effect: An example from Addis Ababa', Landscape and Urban Planning, 123, pp. 87–95. Available at: https://doi.org/10.1016/j.landurbplan.2013.12.008.

Fletcher, T.D. et al. (2015) 'SUDS, LID, BMPs, WSUD and more – The evolution and application of terminology surrounding urban drainage', Urban Water Journal, 12(7), pp. 525–542. Available at: https://doi.org/10.1080/1573062X.2014.916314;WGROUP:STRING:PUBLICATION.

Franklin, S.E. et al. (2000) 'Incorporating texture into classification of forest species composition from airborne multispectral images', International Journal of Remote Sensing, 21(1), pp. 61–79. Available at: https://doi.org/10.1080/014311600210993;WEBSITE:WEBSITE:TFOPB;PAGEGROUP:STRING:PUBLICATION.

Gan, Z. et al. (2016) 'A random forest based method for urban object classification using lidar data and aerial imagery', International Conference on Geoinformatics, 2016, p. 7378621. Available at: https://doi.org/10.1109/GEOINFORMATICS.2015.7378621.

Gao, T. et al. (2015) 'Mapping Spatial Distribution of Larch Plantations from Multi-Seasonal Landsat-8 OLI Imagery and Multi-Scale Textures Using Random Forests', Remote Sensing 2015, Vol. 7, Pages 1702-1720, 7(2), pp. 1702–1720. Available at: https://doi.org/10.3390/RS70201702.

Ghimire, B., Rogan, J. and Miller, J. (2010) 'Contextual land-cover classification: Incorporating spatial dependence in land-cover classification models using random forests and the Getis statistic', Remote Sensing Letters, 1(1), pp. 45–54. Available at: https://doi.org/10.1080/01431160903252327;WEBSITE:WEBSITE:TFOPB;PAGEGROUP:STRING:PUBLICATION.

Gill, S.E. et al. (2007) 'Adapting cities for climate change: The role of the green infrastructure', Built Environment, 33(1), pp. 115–133. Available at: https://doi.org/10.2148/benv.33.1.115.

Gislason, P.O., Benediktsson, J.A. and Sveinsson, J.R. (2006) 'Random forests for land cover classification', Pattern Recognition Letters, 27(4), pp. 294–300. Available at: https://doi.org/10.1016/j.patrec.2005.08.011.

Gündel, H. and Kalaycı Önaç, A. (2025) 'Simulating blue and green infrastructure tools via SWMM in order to prevent flood hazard in an urban area', Natural Hazards, 121(2), pp. 1885–1909. Available at: https://doi.org/10.1007/s11069-024-06868-8.

Halecki, W., Stachura, T. and Fudała, W. (2025) 'Redefining urban spaces in stormwater assessment through ecosystem management: A narrative review', in Ambio. Springer Science and Business Media B.V. Available at: https://doi.org/10.1007/s13280-025-02156-2.

Haralick, R.M., Dinstein, I. and Shanmugam, K. (1973) 'Textural Features for Image Classification', IEEE Transactions on Systems, Man and Cybernetics, SMC(6), pp. 610–621. Available at: https://doi.org/10.1109/TSMC.1973.4309314.
He, C. et al. (2010) 'Improving the normalized difference built-up index to map urban built-up areas using a semi-automatic segmentation approach', Remote Sensing Letters, 1(4), pp. 213–221. Available at: https://doi.org/10.1080/01431161.2010.481681.

Hoang, N.D. and Tran, X.L. (2021) 'Remote Sensing-Based Urban Green Space Detection Using Marine Predators Algorithm Optimized Machine Learning Approach', Mathematical Problems in Engineering, 2021, p. 5586913. Available at: https://doi.org/10.1155/2021/5586913.

Ignatieva, M. and Mofrad, F. (2023) 'Understanding Urban Green Spaces Typology's Contribution to Comprehensive Green Infrastructure Planning: A Study of Canberra, the National Capital of Australia', Land, 12(5), p. 950. Available at: https://doi.org/10.3390/land12050950.

Isaac, E., Easwarakumar, K.S. and Isaac, J. (2017) 'Urban landcover classification from multispectral image data using optimized AdaBoosted random forests', Remote Sensing Letters, 8(4), pp. 350–359. Available at: https://doi.org/10.1080/2150704X.2016.1274443.

Istanbul Planning Agency - IPA (2023) Kentsel Dönüşüm Yasa Değişikliği: Dönüşüm Kimin İçin? Istanbul.

Jeevalakshmi, D., Reddy, S.N. and Manikiam, B. (2016) 'Land cover classification based on NDVI using LANDSAT8 time series: A case study Tirupati region', International Conference on Communication and Signal Processing, ICCSP 2016, pp. 1332–1335. Available at: https://doi.org/10.1109/ICCSP.2016.7754369.

Jia, J., Cui, W. and Liu, J. (2022) 'Urban Catchment-Scale Blue-Green-Gray Infrastructure Classification with Unmanned Aerial Vehicle Images and Machine Learning Algorithms', Frontiers in Environmental Science, 9, p. 778598. Available at: https://doi.org/10.3389/fenvs.2021.778598.

Kayitakire, F., Hamel, C. and Defourny, P. (2006) 'Retrieving forest structure variables based on image texture analysis and IKONOS-2 imagery', Remote Sensing of Environment, 102(3–4), pp. 390–401. Available at: https://doi.org/10.1016/J.RSE.2006.02.022.

Kocabas, A., Gibson, M.S. and Diren, M. (2015) 'Climate change mitigation: From carbon-intensive sprawl toward low carbon urbanization: Progress and prospects for istanbul', in Handbook of Climate Change Adaptation. Springer Berlin Heidelberg, pp. 785–798. Available at: https://doi.org/10.1007/978-3-642-38670-1_35.

Korkmaz, C. and Balaban, O. (2020) 'Sustainability of urban regeneration in Turkey: Assessing the performance of the North Ankara Urban Regeneration Project', Habitat International, 95. Available at: https://doi.org/10.1016/j.habitatint.2019.102081.

Köylüoğlu, Ö. (2015) 'Urban transformation opportunity for sustainable development and benefits based on LCC analysis', IABSE Conference, Geneva 2015: Structural Engineering: Providing Solutions to Global Challenges - Report, pp. 1943–1949. Available at: https://doi.org/10.2749/222137815818359465.

Liu, T. and Yang, X. (2013) 'Mapping vegetation in an urban area with stratified classification and multiple endmember spectral mixture analysis', Remote Sensing of Environment, 133, pp. 251–264. Available at: https://doi.org/10.1016/j.rse.2013.02.020.

Lu, W. et al. (2023) 'Embracing green spaces: Exploring spatiotemporal changes in urban green space accessibility and its equity in Guangzhou, China for sustainable urban greening', Environmental and Sustainability Indicators, 19, p. 100290. Available at: https://doi.org/10.1016/J.INDIC.2023.100290.

Luo, Y. et al. (2021) 'China urbanization process induced vegetation degradation and improvement in recent 20 years', Cities, 114, p. 103207. Available at: https://doi.org/10.1016/j.cities.2021.103207.

Matasov, V. et al. (2020) 'IoT monitoring of urban tree ecosystem services: Possibilities and challenges', Forests, 11(7), p. 775. Available at: https://doi.org/10.3390/F11070775.

Mathey, J. et al. (2015) 'Brownfields As an Element of Green Infrastructure for Implementing Ecosystem Services into Urban Areas', Journal of Urban Planning and Development, 141(3), p. A4015001. Available at: https://doi.org/10.1061/(ASCE)UP.1943-5444.0000275.

Meerow, S. and Newell, J.P. (2017) 'Spatial planning for multifunctional green infrastructure: Growing resilience in Detroit', Landscape and Urban Planning, 159, pp. 62–75. Available at: https://doi.org/10.1016/j.landurbplan.2016.10.005.

Norton, B.A. et al. (2015) 'Planning for cooler cities: A framework to prioritise green infrastructure to mitigate high temperatures in urban landscapes', Landscape and Urban Planning, 134, pp. 127–138. Available at: https://doi.org/10.1016/j.landurbplan.2014.10.018.

Nowak, D.J., Crane, D.E. and Stevens, J.C. (2006) 'Air pollution removal by urban trees and shrubs in the United States', Urban Forestry and Urban Greening, 4(3–4), pp. 115–123. Available at: https://doi.org/10.1016/j.ufug.2006.01.007.

Ogwu, M.C. et al. (2025) 'Green Infrastructure and Environmental Health Security: The Role of Nature-Based Solutions in Improving Urban Health', in Environmental Science and Engineering. Springer Science and Business Media Deutschland GmbH, pp. 225–255. Available at: https://doi.org/10.1007/978-3-031-81966-7_9.

Oke, T.R. (1989) 'The micrometeorology of the urban forest', Philosophical Transactions of the Royal Society of London. B, Biological Sciences, 324(1223), pp. 335–349. Available at: https://doi.org/10.1098/RSTB.1989.0051.
Pacifici, F., Chini, M. and Emery, W.J. (2009) 'A neural network approach using multi-scale textural metrics from very high-resolution panchromatic imagery for urban land-use classification', Remote Sensing of Environment, 113(6), pp. 1276–1292. Available at: https://doi.org/10.1016/J.RSE.2009.02.014.

Pauleit, S. et al. (2019) 'Advancing urban green infrastructure in Europe: Outcomes and reflections from the GREEN SURGE project', Urban Forestry & Urban Greening, 40, pp. 4–16. Available at: https://doi.org/10.1016/J.UFUG.2018.10.006.

Pitman, S.D., Daniels, C.B. and Ely, M.E. (2015) 'Green infrastructure as life support: Urban nature and climate change', Transactions of the Royal Society of South Australia, 139(1), pp. 97–112. Available at: https://doi.org/10.1080/03721426.2015.1035219.

Rahaman, M. et al. (2025) 'Combining deep learning and machine learning techniques to track air pollution in relation to vegetation cover utilizing remotely sensed data', Journal of Environmental Management, 376, p. 124323. Available at: https://doi.org/10.1016/j.jenvman.2025.124323.

Ramyar, R., Ackerman, A. and Johnston, D.M. (2021) 'Adapting cities for climate change through urban green infrastructure planning', Cities, 117, p. 103316. Available at: https://doi.org/10.1016/J.CITIES.2021.103316.

Rodriguez-Galiano, V.F., Ghimire, B., et al. (2012) 'An assessment of the effectiveness of a random forest classifier for land-cover classification', ISPRS Journal of Photogrammetry and Remote Sensing, 67(1), pp. 93–104. Available at: https://doi.org/10.1016/j.isprsjprs.2011.11.002.

Rodriguez-Galiano, V.F., Chica-Olmo, M., et al. (2012) 'Random Forest classification of Mediterranean land cover using multi-seasonal imagery and multi-seasonal texture', Remote Sensing of Environment, 121, pp. 93–107. Available at: https://doi.org/10.1016/J.RSE.2011.12.003.

Russo, A. and Cirella, G.T. (2018) 'Modern Compact Cities: How Much Greenery Do We Need?', International Journal of Environmental Research and Public Health 2018, Vol. 15, Page 2180, 15(10), p. 2180. Available at: https://doi.org/10.3390/IJERPH15102180.

Sarker, L.R. and Nichol, J.E. (2011) 'Improved forest biomass estimates using ALOS AVNIR-2 texture indices', Remote Sensing of Environment, 115(4), pp. 968–977. Available at: https://doi.org/10.1016/J.RSE.2010.11.010.

Schilling, J. and Logan, J. (2008) 'Greening the rust belt: A green infrastructure model for right sizing America's shrinking cities', Journal of the American Planning Association, 74(4), pp. 451–466. Available at: https://doi.org/10.1080/01944360802354956;PAGE:STRING:ARTICLE/CHAPTER.

Semeraro, T., Aretano, R. and Pomes, A. (2017) 'Green Infrastructure to Improve Ecosystem Services in the Landscape Urban Regeneration', IOP Conference Series: Materials Science and Engineering, 245(8), p. 082044. Available at: https://doi.org/10.1088/1757-899X/245/8/082044.

Senosiain, J.L. (2020) 'Urban regreeneration: Green urban infrastructure as a response to climate change mitigation and adaptation', International Journal of Design and Nature and Ecodynamics, 15(1), pp. 33–38. Available at: https://doi.org/10.18280/ijdne.150105.

Shi, D. and Yang, X. (2017) 'A relative evaluation of random forests for land cover mapping in an Urban Area', Photogrammetric Engineering and Remote Sensing, 83(8), pp. 541–552. Available at: https://doi.org/10.14358/PERS.83.8.541.

Spronken-Smith, R.A. and Oke, T.R. (1999) 'Scale modelling of nocturnal cooling in urban parks', Boundary-Layer Meteorology, 93(2), pp. 287–312. Available at: https://doi.org/10.1023/A:1002001408973/METRICS.

T. C. Resmi Gazete (2012) Afet Riski Altındaki Alanların Dönüştürülmesi Hakkında Kanun. Türkiye: https://resmigazete.gov.tr/eskiler/2012/05/20120531-1.htm.

Talukdar, S. et al. (2020) 'Land-use land-cover classification by machine learning classifiers for satellite observations-A review', Remote Sensing. MDPI AG. Available at: https://doi.org/10.3390/rs12071135.

Turk, S.S., Tarakci, S. and Gürsoy, N. (2020) 'A large-scale urban renewal project in a vicious cycle of commons and anticommons: The Fikirtepe case (Istanbul, Turkey)', Habitat International, 102, p. 102209. Available at: https://doi.org/10.1016/J.HABITATINT.2020.102209.

Tzoulas, K. et al. (2007) 'Promoting ecosystem and human health in urban areas using Green Infrastructure: A literature review', Landscape and Urban Planning, 81(3), pp. 167–178. Available at: https://doi.org/10.1016/j.landurbplan.2007.02.001.

Unser, M. (1995) 'Texture Classification and Segmentation Using Wavelet Frames', IEEE Transactions on Image Processing, 4(11), pp. 1549–1560. Available at: https://doi.org/10.1109/83.469936.

Weng, Q., Lu, D. and Schubring, J. (2004) 'Estimation of land surface temperature-vegetation abundance relationship for urban heat island studies', Remote Sensing of Environment, 89(4), pp. 467–483. Available at: https://doi.org/10.1016/j.rse.2003.11.005.

Wolch, J.R., Byrne, J. and Newell, J.P. (2014) 'Urban green space, public health, and environmental justice: The challenge of making cities "just green enough"', Landscape and Urban Planning, 125, pp. 234–244. Available at: https://doi.org/10.1016/j.landurbplan.2014.01.017.

World Health Organization - WHO (2012) Health indicators of sustainable cities in the context of the Rio+ 20 UN Conference on Sustainable Development. Geneva, Switzerland: OECD. Available at: https://doi.org/10.1787/9789264122246-en.

Wu, Q. et al. (2019) 'Land-cover classification using GF-2 images and airborne lidar data based on Random Forest', International Journal of Remote Sensing, 40(5), pp. 2410–2426. Available at: https://doi.org/10.1080/01431161.2018.1483090.

Yağçı, E. (2025) 'Subterranean eco-dystopia in Istanbul: the concreted segregation of Tarlabaşı', Local Environment, 30(2), pp. 207–230. Available at: https://doi.org/10.1080/13549839.2024.2422369.

Yalazi, B. et al. (2017) 'Urban regeneration with carbon economy', WIT Transactions on Ecology and the Environment, 223, pp. 125–133. Available at: https://doi.org/10.2495/SC170111.

Yan, W.Y., Shaker, A. and El-Ashmawy, N. (2015) 'Urban land cover classification using airborne LiDAR data: A review', Remote Sensing of Environment, 158, pp. 295–310. Available at: https://doi.org/10.1016/J.RSE.2014.11.001.

Yazar, M. et al. (2020) 'From urban sustainability transformations to green gentrification: urban renewal in Gaziosmanpaşa, Istanbul', Climatic Change, 160(4), pp. 637–653. Available at: https://doi.org/10.1007/s10584-019-02509-3.
Yenidünya, S.S. and Limoncu, S. (2024) 'Cost effective design decision model for sustainable building renewal[Sürdürülebilir bina yenilemeye ilişkin maliyet etkin tasarım karar modeli]', Journal of the Faculty of Engineering and Architecture of Gazi University, 39(4), pp. 2497–2514. Available at: https://doi.org/10.17341/gazimmfd.1294986.

Yuan, F. and Bauer, M.E. (2007) 'Comparison of impervious surface area and normalized difference vegetation index as indicators of surface urban heat island effects in Landsat imagery', Remote Sensing of Environment, 106(3), pp. 375–386. Available at: https://doi.org/10.1016/j.rse.2006.09.003.

Zha, Y., Gao, J. and Ni, S. (2003) 'Use of normalized difference built-up index in automatically mapping urban areas from TM imagery', International Journal of Remote Sensing, 24(3), pp. 583–594. Available at: https://doi.org/10.1080/01431160304987.

Zhang, J. et al. (2025) 'A strategy for green infrastructure network based on multifunctional synergy', Ecological Frontiers, 45(2), pp. 483–496. Available at: https://doi.org/10.1016/j.ecofro.2024.11.013.

Appendix

Table A. 1. Sample set of the study (n=21).

No.	**Project Site**	**District**	**Area Size (ha)**
1	Demirkapı	Bağcılar	4.73
2	Evren	Bağcılar	1.74
3	Çınar, İnönü, Sancaktepe, Yavuzselim, Merkez	Bağcılar	22.07
4	İstiklal	Beyoğlu	8.8
5	Örnektepe, Sütlüce	Beyoğlu	2.5
6	Havaalanı	Esenler	7.18
7	Oruçreis 2	Esenler	4.65
8	Alibeyköy	Eyüpsultan	2.36
9	Çırçır 2	Eyüpsultan	1.52
10	Sarıgöl	Gaziosmanpaşa	5.83
11	Karabekir, Fevziçakmak	Gaziosmanpaşa	59.03
12	Sarıgöl, Yenidoğan	Gaziosmanpaşa	33.17
13	Bağlarbaşı	Gaziosmanpaşa	16.6
14	Yıldız Tabya 1. Kısım	Gaziosmanpaşa	14.16
15	Fikirtepe 1	Kadıköy	98.73
16	Fikirtepe 2	Kadıköy	35.61
17	Yahya Kemal	Kağıthane	3.39
18	Kaynarca	Pendik	5.24
19	İçmeler	Tuzla	6.78
20	Sümer	Zeytinburnu	3.8
21	Beştelsiz	Zeytinburnu	0.5

Table A. 2. Selected regeneration sites.

	Site-1	Site-2	Site3
	Karabekir, Fevziçakmak	Fikirtepe	Çınar, İnönü, Sancaktepe, Yavuzselim, Merkez
Pre-regeneration			
Population Capacity	13,615	40,439	3,363
Num. of Buildings	917	4,035	277
Num. of Wokplace Untis	388	2,384	0
Construction Area (M2)	558,508.31	903,056.10	218,912.00
Post-regeneration			
Population Capacity	18291	70,563	6,674
Num. of Buildings	844	840	230
Num. of Wokplace Untis	300	2,238	987
Construction Area (M2)	662,296.14	9,032,574.66	295,026.00
Current Population (2023)	15,681	9,129	5,451
Area Size (Ha)	59.03	98.73	22.07
Num. of Demolished Building	134	3,236	57
Num. of New Buildings	24	143	6

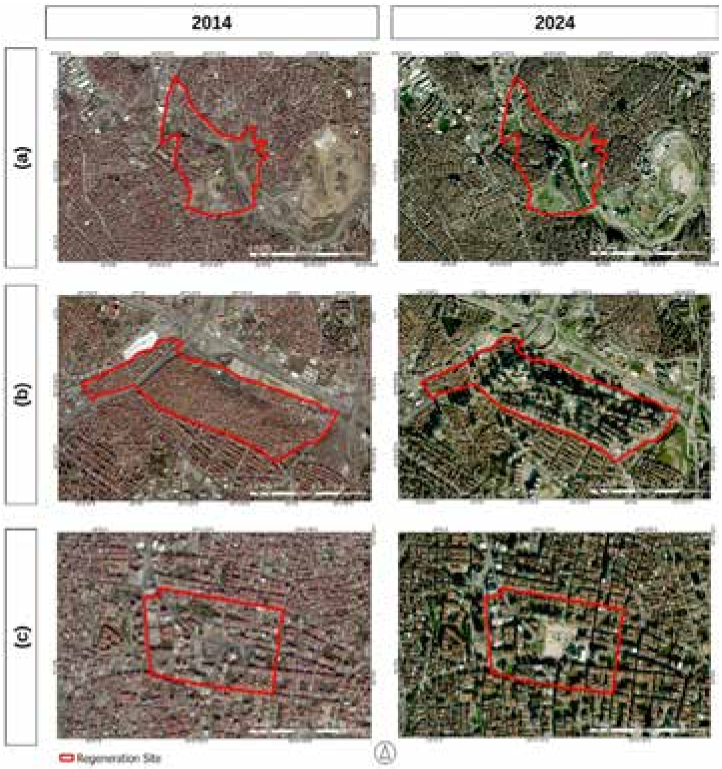

Figure A. 1. Study areas in 2014 and 2024: (a) Site – 1, Karabekir, Fevziçakmak – Gaziosmanpaşa; (b) Site – 2, Fikirtepe – Kadıköy; (c) Site – 3, Çınar, İnönü, Sancaktepe, Yavuzselim, Merkez – Bağcılar.